

Assessing Tectonic Plate Reconstruction Models Using Trends in Global Geochemical Data

Thesis submitted in accordance with the requirements of the University of
Adelaide for an Honours Degree in Geophysics

Benjamin John Forrest

November 2020



THE UNIVERSITY
of ADELAIDE

ASSESSING TECTONIC PLATE RECONSTRUCTION MODELS USING TRENDS IN GLOBAL GEOCHEMICAL DATA

PLATE RECONSTRUCTIONS AND GLOBAL GEOCHEMICAL DATA

ABSTRACT

The evolution of Earth's crust is a complex four-dimensional framework. Tectonic plate reconstruction models aim to constrain the global positions and movements of plates through Earth's history. These models are vital for understanding various Earth processes, theories and phenomenon. Models for relatively recent geological time are well-constrained, however, the further back in time we aim to reconstruct, the more uncertainty arises in models produced. This causes models for the same point in time to have differing configuration hypotheses. Further methods are hence needed to improve and validate proposed models. This study makes use of a vast global geochemical database with over one million samples. Data is grouped into pre-defined geological provinces. Data is normalised based on the type of province it falls into, in terms of its tectonic setting. Province trace geochemical data is then statistically analysed and compared to other provinces in order to determine conjugate province pairs. Reconstructions of Pangea are used to determine known province pairs. Trace geochemistry trends are then assessed across these known pairs via hypothesis testing, yielding a p-value test statistic signifying similarity between province geochemistry. Unrelated province geochemistry is also assessed as a control case for which p-values are also determined. P-value thresholds are defined for each trace element. Hypothesis testing between two provinces geochemistry yielding a p-value higher than this threshold signifies a geochemical similarity between provinces unique to conjugate pairs. Using this method, conjugate province pairs for the North China Craton during the Paleoproterozoic are identified. The results from these tests have implications for the configuration of the supercontinent Nuna. Ultimately, the methods employed in this study emphasise the importance of geochemical data in constraining the configuration of continental blocks within past supercontinents and hence plate reconstruction models.

KEYWORDS

Plate reconstruction, hypothesis testing, conjugate province

TABLE OF CONTENTS

Assessing Tectonic Plate Reconstruction Models Using Trends In Global Geochemical Data.....	i
Plate Reconstructions and Global Geochemical Data	i
Abstract.....	i
Keywords.....	i
List of Figures and Tables	2
Introduction and Background	4
Methods	7
Database Overview.....	7
Filtering and Pre-processing.....	10
Hypothesis Testing Method Validation of Known Conjugate Provinces.....	10
Using Hypothesis Testing to Identify Conjugate Provinces.....	15
Results	17
Validation of Method by Evaluating Pangea Conjugate Pairs	17
Identification of Known Conjugate Province Pairs	17
Comparison of Age Distributions.....	22
Two-Sample T-test Evaluation.....	22
Two-Sample Kolmogorov-Smirnov test Evaluation	24
Identifying Conjugate Province Pairs for North China Craton during Nuna	26
North China Craton Hypothesis Testing	26
North China Craton Age Distribution Comparisons	27
Discussion.....	27
Interpretation of Nuna Configuration Result.....	27
Critique of Hypothesis Testing.....	29
Suitability of Using Geochemical Data for Plate Reconstructions.....	32
Conclusions	33
Acknowledgments	35
References	35

LIST OF FIGURES AND TABLES

Figure 1: The 4 main hypotheses for the connection between Australia, East Antarctica and Laurentia during the assembly of the supercontinent Rodinia in the Proterozoic: a) SWEAT (South Western U.S. with East Antarctica) model (Dalziel, 1997; Hoffman, 1991; Moores, 1991), b) AUSWUS (Australia with south western U.S.) model (Brookfield, 1993; Burrett & Berry, 2000; Karlstrom et al., 1999), c) AUSMEX (Australia with Mexico) model (Wingate & Giddings, 2000) and d) “The missing link” (South China between Laurentia and Australia) model (Li et al., 2008; Li et al., 1995). 5

Figure 2: Diagrams showcasing the breakup of a hypothetical supercraton and how various geological features can be used as piercing points for reconstruction modified from (Ernst & Bleeker, 2010). a) a supercraton just prior to breakup due to thermal perturbation from a hotspot, b) rifting has been successful, meaning there are now two smaller cratons, which host several geological features which can be used to infer configuration before breakup, c) the further breakup into three cratons, with some features being lost due to differential uplift and erosion and d) a reconstruction of the configuration of the original supercraton based on the available evidence..... 7

Figure 3: Histogram displaying the temporal distribution of the data in both the global geochemical database and the supplementary zircon geochronology database (Puetz, 2018)..... 9

Figure 4: Maps displaying both the spatial density of data on the global scale and all province polygons within the database, outlined in black (data is also coloured according to provinces). 9

Figure 5: Screenshot of the GPLates software with the Meredith et al. 2019 model uploaded. Overlain on the continental blocks are the provinces for the South American and African continents. Time slice is given in the top left corner (100 Ma)..... 11

Figure 6: Four plots which give a visual summary as to how the normalisation process works: a) distribution of log Uranium concentration for an arbitrary province (Ruby Terrane in north-western North America), b) plot of log Uranium concentration vs silica (wt.%) for all data of the same province type as Ruby Terrane, in this case, orogenic belts (shown in black), with a smoothed model of quantile curves (in blue), which have been fit by grouping data into 2 wt.% silica bins and fitting ideal scale parameters (mean and standard deviation) to each bin, c) smooth quantile curves with Ruby Terrane of log Uranium concentration distribution overlain and d) data distributions before and after normalisation process, showing a decrease in the mean of the distribution. 13

Figure 7: Simplified flowchart summarising the methodology behind using hypothesis testing to compare the trace element geochemistry of identified and suspected conjugate province pairs. 16

Figure 8: Kernel density plots displaying comparisons in the age distributions of the 20 most significant identified known conjugate province pairs in terms of hypothesis testing. All x-axis range from present day to 2500 Ma (data younger than age of separation was filtered out for hypothesis testing). 22

Figure 9: p-value histograms of T hypothesis testing for the Heavy Rare Earth Elements. Blue dataset signifies identified known conjugate province pairs, while orange dataset signifies random province pairing. Histograms are fitted to an ideal probability density function (blue line is known pairs, red line is controls). Identified thresholds have also been plotted (black dashed line)..... 23

Figure 10: the 20 conjugate province pairs identified, coloured by how well their trace geochemistry distributions match relative to all other pairs (red signifies a good match, blue signifies a poorer match but are still significant matches in absolute terms). Derived from T hypothesis testing. Lines connect the pairs, while a circle highlights the Arabian-Nubian Shield pairs, an ideal case. 24

Figure 11: p-value histograms of K-S hypothesis testing for the Heavy Rare Earth Elements. Blue dataset signifies identified known conjugate province pairs, while orange dataset signifies random province pairing. Histograms are fitted to an ideal probability density function (blue line is known pairs, red line is controls). Identified thresholds have also been plotted (black dashed line). 25

Figure 12: the 20 conjugate province pairs identified, coloured by how well their trace geochemistry distributions match relative to all other pairs (red signifies a good match, blue signifies a poorer match but are still significant matches in absolute terms). Derived from K-S hypothesis testing. Lines connect the pairs, while a circle highlights the Arabian-Nubian Shield pairs, an ideal case. 26

Figure 13: The 26 provinces which significantly pass both T and K-S hypothesis testing, coloured by how well their trace geochemistry distributions compare to the North China Craton provinces (red signifies a good match, blue signifies a poorer match but still passes all tests). Yellow regions are cratonic fragments of the crust which were all postulated to have been part of the Nuna supercontinent, which have been labelled. ... 26

Figure 14: Kernel density plots displaying comparisons of age distributions for: a) the six provinces making up the North China Craton, b) the three Indian provinces which pass hypothesis testing, c) the two North Australian Craton provinces which pass hypothesis testing, d) the two Baltica provinces which pass hypothesis testing, e) the two Siberian provinces which pass hypothesis testing and f) the three South American provinces which pass hypothesis testing. All x-axis range from 1000 Ma to 3000 Ma. 27

Figure 15: Several proposed relative configurations for the supercontinent Nuna (Columbia) during the late Paleoproterozoic, modified from (de Oliveira Chaves & de Rezende, 2019). Models were given by: a) (Rogers & Santosh, 2002, 2009), b) (Zhao et al., 2002; Zhao et al., 2004), c) (Hou et al., 2008), d) (Zhang et al., 2012), e) (Pisarevsky et al., 2014) and f) (de Oliveira Chaves & de Rezende, 2019). 29

Figure 16: Hypothesis testing for two arbitrary synthetic normal distributions, with number of data for both sets changing (sample size for both distributions seen above subplots). Both distributions have the same standard deviation (0.2), however, their means differ (blue set has a mean of 5, purple set has a mean of 5.1). Green background represents a failure to reject the null hypothesis, whereas red background represents rejection of the null hypothesis, for both T and K-S testing. 31

INTRODUCTION AND BACKGROUND

Tectonic plate reconstructions yield insights into past configurations of the Earth's continental crust. Reconstruction models are created by using multiple types of geological data and observations, both quantitative and qualitative, which are usually sourced from large dataset compilations (Cawood et al., 2006; Domeier & Torsvik, 2014; Schiffer et al., 2015). Collaboration from several disciplines in Earth science is generally needed. These models are vital for understanding the geodynamics and kinematics of Earth's tectonic plates through time and are relevant to all fields of geological and geophysical studies in a global context (Evans et al., 2016; Merdith et al., 2017).

Reconstructing past plate configurations is especially relevant to the theory of the supercontinent cycle. This is the theory that continental land mass on Earth experiences quasi-cycles of amalgamation, shared stability and dispersal which has punctuated Earth's history since the onset of plate tectonics (Condie, 2002; Rogers & Santosh, 2003; Yoshida & Santosh, 2011). A supercontinent will remain together until there is a perturbation in the stability of the continent, causing it to break-apart and rift. A vast amount of research has gone into reconstructing tectonic plates and assessing their implications for the assembly and breakup of supercontinents through time.

Much research has been conducted into plate reconstruction. The most recent supercontinent, Pangea, has a configuration that is relatively well constrained (Verard, 2019). This is due to the abundance of proxies in geological observations which allow us to reconstruct this supercontinent. However, supercontinents further back in geological time is harder to model due to uncertainties in observations and lack of critical data (Evans, 2013). This results in reconstruction models in the older Earth to

have various differing configuration hypotheses (Nance et al., 2014). For example, the supercontinent Rodinia has several main configuration hypotheses for the connection between the Laurentian and Australian continents (Salminen, 2009). Conjugate margins (defined as continental margins which were once together at some point in time during the amalgamation of a supercontinent) are poorly understood between these two land masses due to multiple propositions for their relative positions during this time. As such, the exact geography of the Rodinia supercontinent is uncertain (Figure 1).

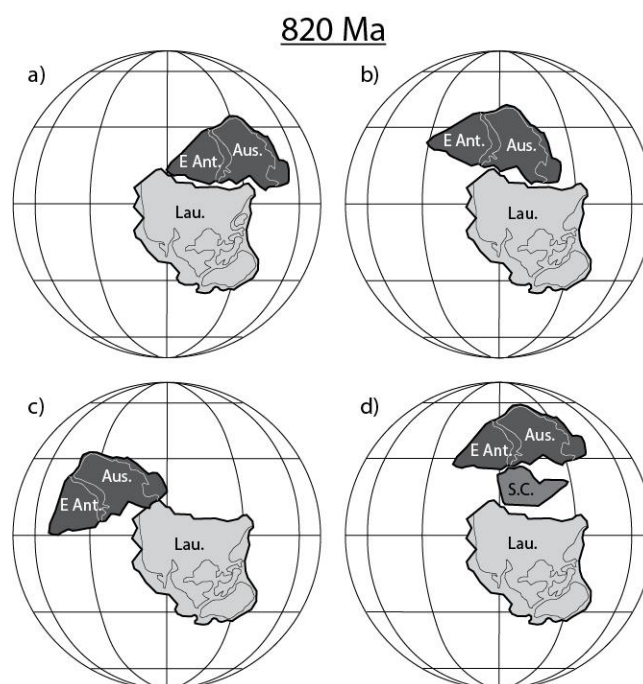


Figure 1: The 4 main hypotheses for the connection between Australia, East Antarctica and Laurentia during the assembly of the supercontinent Rodinia in the Proterozoic: a) SWEAT (South Western U.S. with East Antarctica) model (Dalziel, 1997; Hoffman, 1991; Moores, 1991), b) AUSWUS (Australia with south western U.S.) model (Brookfield, 1993; Burrett & Berry, 2000; Karlstrom et al., 1999), c) AUSMEX (Australia with Mexico) model (Wingate & Giddings, 2000) and d) “The missing link” (South China between Laurentia and Australia) model (Li et al., 2008; Li et al., 1995).

The aims of this project is to determine whether province-scale geochemical concentrations can be used to accurately identify conjugate terranes, which has applications in validating or improving tectonic reconstructions. It is postulated that conjugate provinces share similar trends in trace element geochemistry, such that when trace element distributions are compared through hypothesis testing, the test statistic

returns a statistically significant result. Age distributions for these provinces should also significantly match. If indeed conjugate province pass statistical tests, then it is reasonable to assume that this method is applicable in plate reconstruction modelling. For the purposes of this study, a province is hereby defined as a region of the Earth's crust which has a consistent genetic and tectonic history.

Plate reconstructions use the following methods as constraints:

- Paleomagnetic data, which constrains movement of plate, as well as paleo latitudes (Salminen, 2009)
- Matching structural features such as dyke swarms and orogenic belts
- Geological comparisons, which has recently been emphasised to be just as important as quantitative data (White et al., 2013)
- Comparison of lithofacies at passive margins (Salminen, 2009)
- Assessing age data “barcodes” of igneous suites as well as their geochemistry (Ernst & Bleeker, 2010; Ernst et al., 2013)

A visual summary of these methods can be seen in Figure 2.

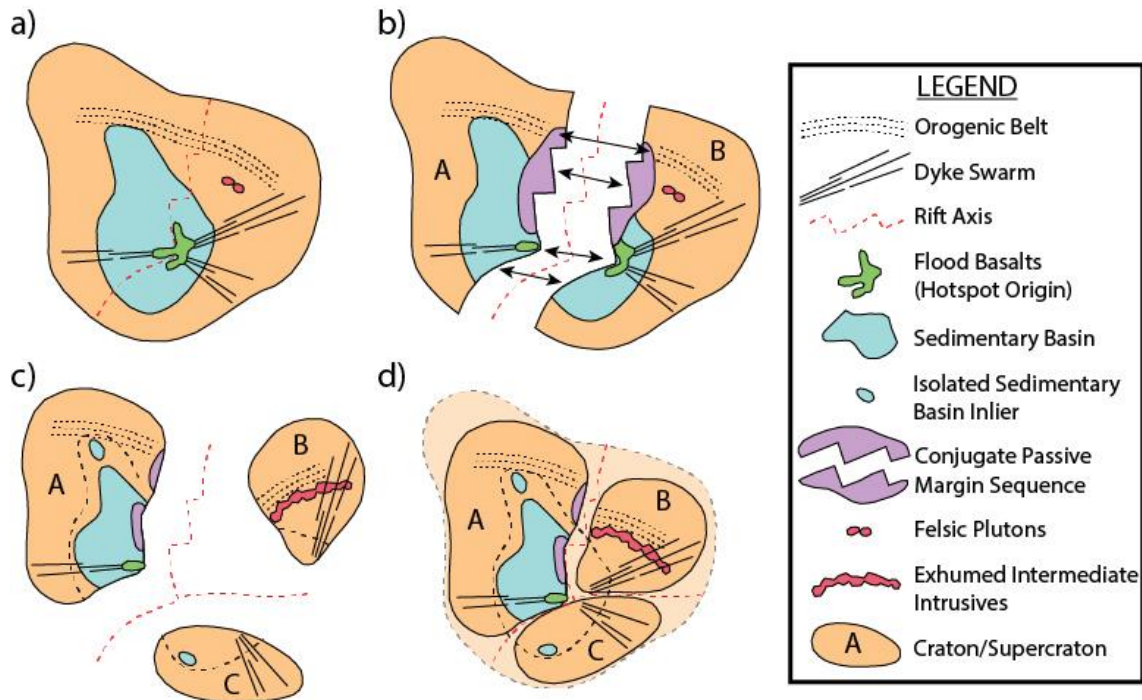


Figure 2: Diagrams showcasing the breakup of a hypothetical supercraton and how various geological features can be used as piercing points for reconstruction modified from (Ernst & Bleeker, 2010). a) a supercraton just prior to breakup due to thermal perturbation from a hotspot, b) rifting has been successful, meaning there are now two smaller cratons, which host several geological features which can be used to infer configuration before breakup, c) the further breakup into three cratons, with some features being lost due to differential uplift and erosion and d) a reconstruction of the configuration of the original supercraton based on the available evidence.

METHODS

Database Overview

The global geochemical database contains 1032591 samples currently. Each sample ideally contains the following information: geographic location (latitude and longitude), rock identification information (rock type, rock name and sample description), major and trace element concentrations, all commonly used isotope ratios, age and age error, computed rock properties (such as density, seismic wave velocity and heat production) and finally data source information (Gard et al., 2019). Not all data points contain information in each of these fields. However, not all of these fields are accounted for in every single sample. The dataset itself was compiled from other geochemical databases

(Gard et al., 2019; Haus & Pauk, 1993; Honarvar et al., 2013; Newfoundland et al., 1999; Sarbas, 2008). Important to this project is the spatial and temporal distribution for the data. As previously mentioned, not all fields for every sample contain information, and the size of the database is reduced by a half when extracting samples with age data. Furthermore, there is a strong bias for number of samples which have ages younger than 100 Ma, where that database reduces significantly in terms of ages the further back into geological time. Because of this, a supplementary geochronology database is used. This database contains Pb/U and Pb/Pb zircon geochronology for igneous, sedimentary and modern sediment samples (Puetz, 2018). Obviously, these samples are not tied to samples in the global geochemical database. However, for the purposes of this study, age information is only needed for provinces and not individual data points and so this secondary database supplements the global geochemical database's age data in order to create age distributions for provinces. An overview of the temporal distribution of the global geochemical database and the supplementary geochronology database is seen in Figure 3.

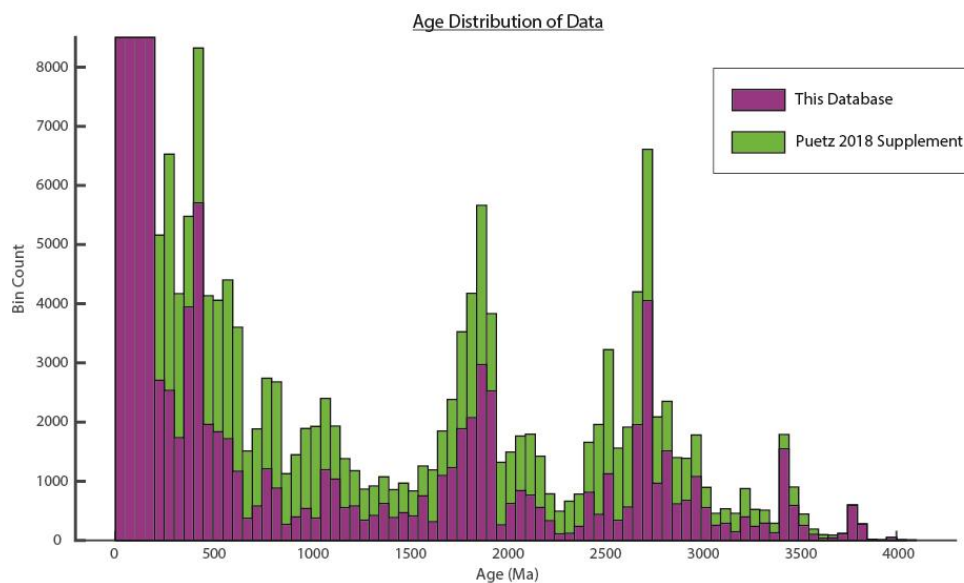


Figure 3: Histogram displaying the temporal distribution of the data in both the global geochemical database and the supplementary zircon geochronology database (Puetz, 2018).

Spatially, the global geochemical database is relatively heterogeneous. Sample numbers are biased toward the North American continent, especially the west coast, and continents like Australia and Asia also have considerably more data than other continents. Also, province polygons are based on geological terranes of consistent tectonic and genetic histories, however this means that province polygons vary greatly in size, both for a singular continent, and across continents. An overview of the spatial distribution of the global geochemical database is seen in Figure 4.

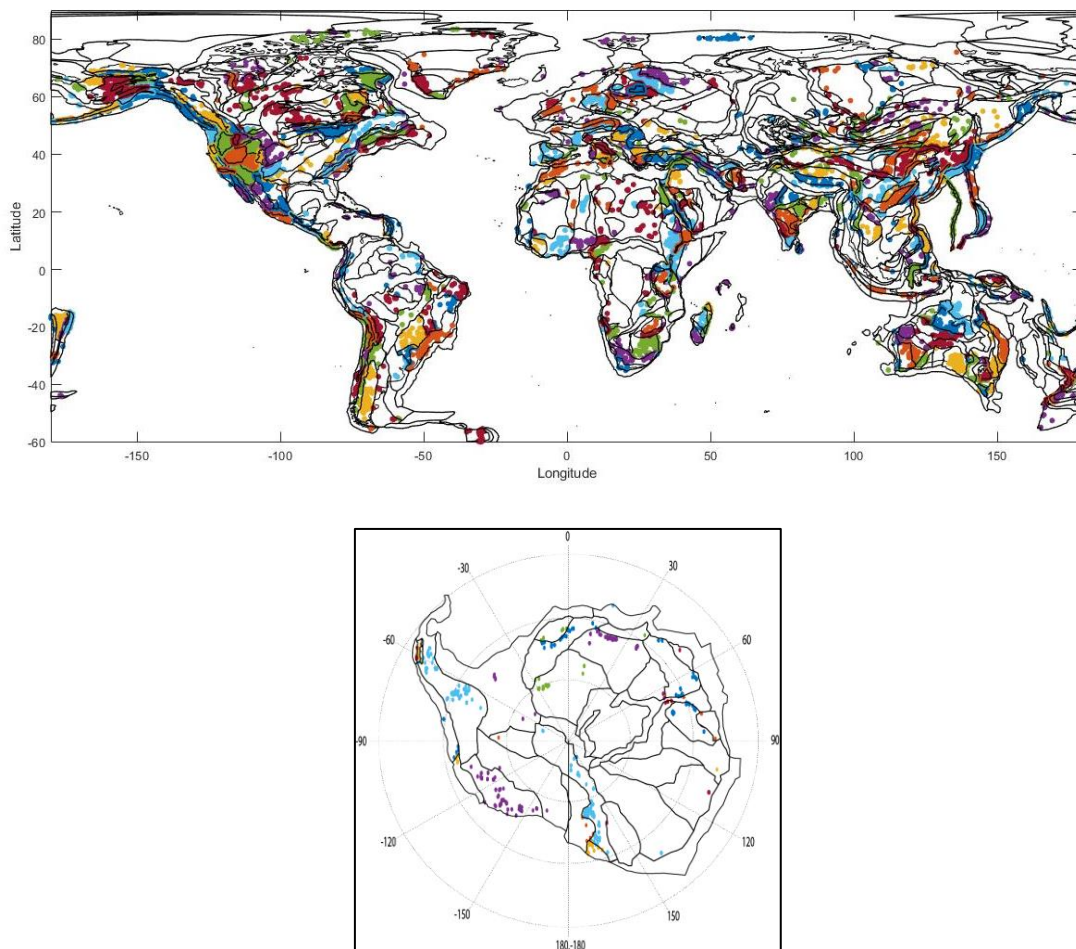


Figure 4: Maps displaying both the spatial density of data on the global scale and all province polygons within the database, outlined in black (data is also coloured according to provinces).

Filtering and Pre-processing

When loading the database in MATLAB[®], a series of pre-processing steps are performed. These steps include: converting all Iron (Fe) concentrations to FeO, assessing below detection limit concentrations in order to maximise available data, making age corrections to the data, assigning rock classifications (both igneous and sedimentary) to each sample through modelling by assessing geochemistry (Hasterok et al., 2019; Hasterok & Webb, 2017), assigning metamorphic facies and finally computing rock properties for each sample, such as heat production, thermal conductivity, density and seismic velocity.

Hypothesis Testing Method Validation of Known Conjugate Provinces

Determining the suitability of testing conjugate province geochemistry must be considered if we are to use those methods to analyse disputed continental configurations. Since the configuration of the most recent supercontinent, Pangea, is so well constrained, we can test trends across known conjugate province pairs. For the purposes of this study, we only assess trace elemental concentrations. A summary of the validation process is as follows:

1. Using the software GPlates, upload a reconstruction model for the last 1 Ga which is recent and generally accepted (Merdith et al., 2019). Within these files are continental polygons, upon which any geospatial element can be “anchored” to, essentially reconstructing their global position for the last billion years with respect to the 1 Ga model. Once uploaded, add the global geochemical database province polygons and anchor these polygons to the continental blocks. Using

the model, reconstruct the positions of all provinces to the time period just before the ensuing breakup of Pangea, which is notably 200 Ma (Figure 5).

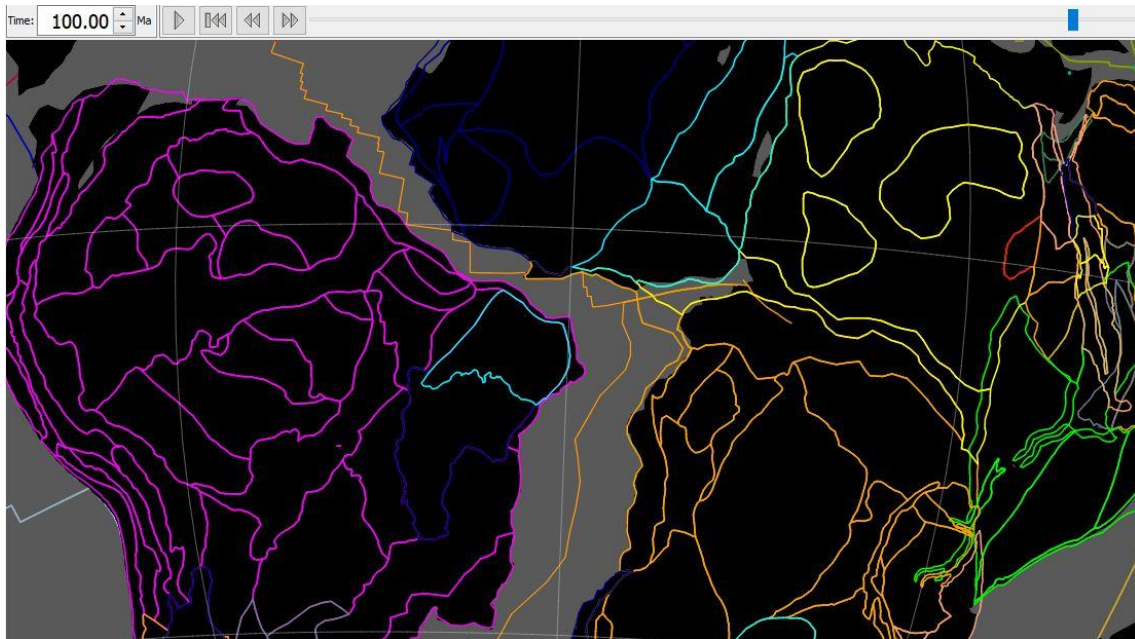


Figure 5: Screenshot of the GPlates software with the Merdith et al. 2019 model uploaded. Overlain on the continental blocks are the provinces for the South American and African continents. Time slice is given in the top left corner (100 Ma).

2. Using both the reconstructed province locations and also literature as supplementary information, identify conjugate margins and hence conjugate province pairs. These conjugate margins should be present day passive margins which have had a relatively simple rifting history since Pangea breakup. Once conjugate province pairs have been noted, identify the time of complete separation due to rifting. This age theoretically marks the cessation of a shared tectonic and genetic history in terms of magmatism. Only data which is older than this separation age will hence be tested.
3. For the conjugate province pairs which have been identified, compare the age distributions for both provinces. Similarity in temporal distributions of province data validates a shared genetic history. Age distributions are derived from the global geochemical database but are also supplemented by another considerably-

sized database containing 700598 samples, all with associated Uranium-Lead or Lead-Lead derived ages. This essentially doubles the depth of the global geochemical database age data and while not directly tied to the geochemical database samples, is sufficient to assess the temporal distributions for provinces.

4. The data for each province is then normalised. It is essential to normalise all data as this ensures relative trends are isolated. For example, conjugate provinces may share igneous bodies with an enrichment in a certain element, although one may contain more mafic geology whereas the other may contain more felsic compositions, meaning that in absolute terms, one set may contain a higher concentration in that particular element than the other. Normalising geochemistry ensures that the enrichment is recognised for both sets of rocks and hence will have a higher probability of passing similarity tests.

Normalisation is a complex process in and of itself, involving several steps in order to normalise all geochemical data. Firstly, data is grouped and extracted by province type, which is encoded into all province polygons. Data for each trace element is then compared with a reference species, which is silica content in weight percent. Data is sorted into bins of width 2 wt. % silica. A log normal distribution of data is assumed for each bin, and hence idealised scale parameters (mean and standard deviation) are fit to the empirical distributions for each bin. Quadratic functions are fit to the means for each bin and linear functions are fit to the standard deviations. A smooth distribution model is then able to be fit to the data based on these idealised functions. This produces quantile levels for the trace element data distribution with respect to silica content. From this point, a subset of the data within the normalised data can be

normalised with respect to the smoothed quantile levels, altering the original distribution of trace element data to a more accurate dataset. This method has been recently developed in order to obtain more accurate spider diagrams for igneous rock trace element analysis (Hasterok, 2020, in prep.). This process can be summarised in the figure below (Figure 6).

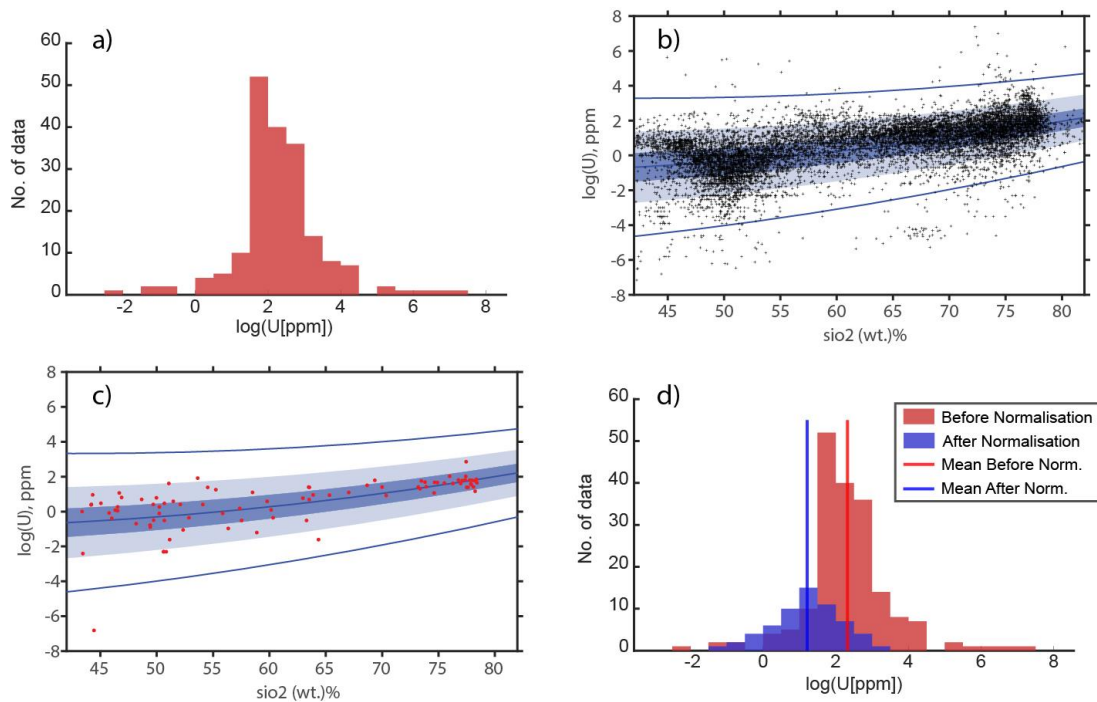


Figure 6: Four plots which give a visual summary as to how the normalisation process works: a) distribution of log Uranium concentration for an arbitrary province (Ruby Terrane in north-western North America), b) plot of log Uranium concentration vs silica (wt.%) for all data of the same province type as Ruby Terrane, in this case, orogenic belts (shown in black), with a smoothed model of quantile curves (in blue), which have been fit by grouping data into 2 wt.% silica bins and fitting ideal scale parameters (mean and standard deviation) to each bin, c) smooth quantile curves with Ruby Terrane of log Uranium concentration distribution overlain and d) data distributions before and after normalisation process, showing a decrease in the mean of the distribution.

5. After normalisation and the other filtering processes, data is now able to be tested. The most suitable way to test similarity between data is statistical testing. This compares the probability density and cumulative density functions between two distributions for a certain element. T-testing assesses the likelihood that two sample distributions have the same mean. F-testing assesses the likelihood that

two sample distributions have the same variance. Kolmogorov-Smirnov testing (K-S testing) tests the similarity in shape of two sample distributions by comparing cumulative distribution functions and assesses likelihood that two Gaussian or non-Gaussian distributions are from the same population.

MATLAB[®] has these statistical test function in-built, meaning the data can be processed automatically. The p-value test statistic gives a quantifiable ranking to distributions based on similarity. Ranging from 0 to 1, a p-value of 0.05 means that there is a 5% probability that a generic sample mean, standard deviation or cumulative density function will be more extreme than the sample distribution in question, meaning that a P-value greater than 0.05 passes the statistical test on the 95% confidence level and hence the null hypothesis that the two sample distributions are drawn from the same population cannot be rejected. The outcome for these tests will be a table of data for each type of statistical test, where each row represents the identified conjugate province pairs and each column represents normalised trace elements, with each cell providing the P-value for each sample distribution test.

6. Once known conjugate province pair distributions are assessed, there is a need to also test unrelated province pairs as a control, to confirm that the passing of a statistical test is unique only to province pairs with definite shared geochemical trends. Assessing the control pairs is relatively simple, where two random, unrelated provinces will be chosen, their geochemical data normalised and statistical tests run in the same way as done for the known conjugate province pairs.

7. Finally, compare the conjugate province pair p-values with the controls.

Theoretically, there should be a clear distinction between the two sets, with the known pairs having higher average P-values when compared to the control average P-values. If this is the case, a threshold can be defined, such that we can confidently say that any province pair which yields a test statistic above the threshold value has a strong possibility of sharing some genetic history in terms of geochemistry. Once validated, any given pair of provinces can be tested and their likelihood of once being joined at some point in time can be assessed.

Using Hypothesis Testing to Identify Conjugate Provinces

Having defined a threshold for t-test and K-S test p-values for each trace element, we can now assess any province pair we suspect are conjugate pairs. Using the same methods of hypothesis testing, we can say that any test for geochemical distributions between two provinces which yields a p-value result higher than the proposed thresholds implies that these provinces are conjugate pairs. Data is filtered for age of separation of the supercontinent we aim to reconfigure. An entire summary of all methods used in this project can be seen in the flowchart in Figure 7.

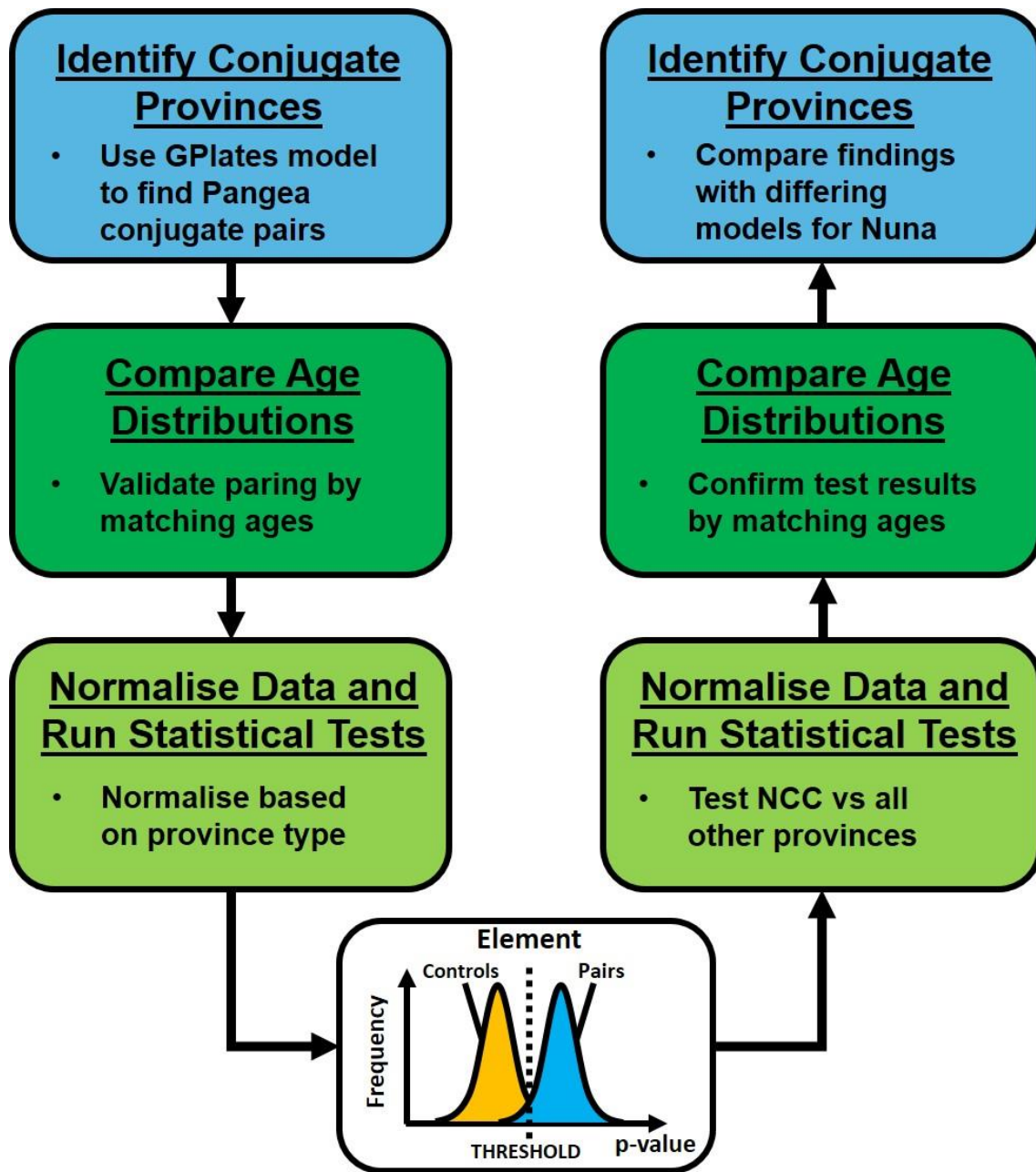


Figure 7: Simplified flowchart summarising the methodology behind using hypothesis testing to compare the trace element geochemistry of identified and suspected conjugate province pairs.

RESULTS

Validation of Method by Evaluating Pangea Conjugate Pairs

IDENTIFICATION OF KNOWN CONJUGATE PROVINCE PAIRS

75 conjugate provinces were identified for the validation procedure. These are summarised in Table 1.

Table 1: All conjugate province pairs identified via the GPlates software and the Meredith et al. 2019 model, which have now rifted. Separation ages are included.

cont	prov_name	conj_cont	conj_name	age_of_separation
africa	South African	south_america	Argentina Volcanic	100
	Rifted Margin		Margin	
africa	South African	south_america	Parana Basin	100
	Rifted Margin			
africa	Cape Fold Belt	south_america	Patagonia Platform	120
africa	Cape Fold Belt	south_america	Bahia Blanca Basin	120
africa	Namaqua-Natal	south_america	Rio de la Plata	120
	Mobile Belt		Craton	
africa	Namaqua-Natal	south_america	Dom Feliciano Belt	120
	Mobile Belt			
africa	Gariiep Belt	south_america	Rio de la Plata	120
			Craton	
africa	Gariiep Belt	south_america	Dom Feliciano Belt	120
africa	Damara	south_america	Dom Feliciano Belt	120
	Orogenic Belt			
africa	Kaoka Belt	south_america	Dom Feliciano Belt	110

africa	Kamanjab Inlier	south_america	Dom Feliciano Belt	110
africa	Angolan Shield	south_america	Dom Feliciano Belt	110
africa	Kaoka Belt	south_america	Mantiqueira Province	110
africa	Kamanjab Inlier	south_america	Mantiqueira Province	110
africa	Angolan Shield	south_america	Mantiqueira Province	110
africa	Central African Margin	south_america	Argentina Volcanic Margin	100
africa	Central African Margin	south_america	Brazil Rifted Margin	100
africa	West Congo and Kimezian Belts	south_america	Mantiqueira Province	100
africa	West Congo and Kimezian Belts	south_america	Sao Francisco Craton	100
africa	Gabon Belt	south_america	Sao Francisco Craton	100
africa	Gabon Belt	south_america	Borborema Province	100
africa	Central African Orogen	south_america	Borborema Province	100
africa	Benin-Nigeria Shield	south_america	Borborema Province	100

africa	Benin-Nigeria Shield	south_america	Media Coreau Domain	100
africa	Leo Rise	south_america	Sao Luis Craton	100
africa	Leo Rise	south_america	Amazonian Graben	100
africa	Kenema-Man Craton	south_america	Amazonian Graben	100
africa	Kenema-Man Craton	south_america	Maroni-Itaciunas Belt	100
africa	Rockelides	south_america	Maroni-Itaciunas Belt	100
africa	Rockelides	north_america	Suwannee Terrane	160
africa	West African Rifted Margin	north_america	West Atlantic Rifted Margin	150
africa	Namaqua-Natal Mobile Belt	antarctica	Ronne Basin	140
africa	Namaqua-Natal Mobile Belt	antarctica	East African Orogen	140
africa	Kaapvaal Craton	antarctica	Grunehogna	140
africa	Kaapvaal Craton	antarctica	East African Orogen	140
africa	Limpopo Belt	antarctica	Grunehogna	140
africa	Limpopo Belt	antarctica	East African Orogen	140
africa	Zimbabwe Craton	antarctica	East African Orogen	140
africa	Barue Complex	antarctica	East African Orogen	140

africa	Mozambique Belt	antarctica	East African Orogen	140
africa	Mozambique Belt	antarctica	Sor Rã,ndone	140
africa	Mozambique Belt	africa	Itremo Block	140
africa	South Azania	africa	Itremo Block	150
africa	South Azania	africa	Antenarivo Block	150
africa	South Azania	africa	Antongil Block	150
africa	Nubian Shield	africa	Arabian Shield	10
africa	Antenarivo Block	india	Southern Granulite Terrane	70
africa	Antongil Block	india	Southern Granulite Terrane	70
africa	Antenarivo Block	india	Western Dharwar Craton	70
africa	Antongil Block	india	Western Dharwar Craton	70
africa	Antongil Block	india	Eastern Dharwar Craton	70
antarctica	Rayner Complex	india	Vijayan Complex	110
antarctica	Rayner Complex	india	Highland Complex	110
antarctica	Rayner Complex	india	Wanni Complex	110
antarctica	Napier Complex	india	Vijayan Complex	110

antarctica	Napier Complex	india	Highland Complex	110
antarctica	Napier Complex	india	Wanni Complex	110
antarctica	Napier Complex	india	Southern Granulite Terrane	110
antarctica	Rayner Complex	india	Eastern Ghats Belt	110
antarctica	Vestfold Craton	india	Bengal Fan	110
antarctica	Albany-Fraser- Wilkes Orogen	australia	Western Yilgarn Craton	40
antarctica	Albany-Fraser- Wilkes Orogen	australia	Eastern Yilgarn Craton	40
antarctica	Albany-Fraser- Wilkes Orogen	australia	Albany-Fraser Orogen	40
antarctica	Mawson Craton	australia	Coompana Province	40
antarctica	Mawson Craton	australia	Gawler Craton	40
antarctica	Terre Adelie Basin	australia	Delamerian Orogen	20
antarctica	Ross Peninsula	australia	Western Tasmania	20
antarctica	Marie Byrd Land	australia	Campbell Plateau	70
africa	Mauritanides	north_america	Suwannee Terrane	160
africa	Mauritanides	north_america	Charleston Arc	160
africa	Mauritanides	north_america	Carolina Terrane	160
africa	Mauritanides	north_america	Meguma Terrane	160
antarctica	Pinjarra Orogen	australia	Western Australian Rifted Margin	40

COMPARISON OF AGE DISTRIBUTIONS

In order to validate that the identified province pairs had a genetic history, age distributions (in the form of kernel density plots) were compared (Figure 8). The number of provinces was reduced to 20 due to insufficient age data.

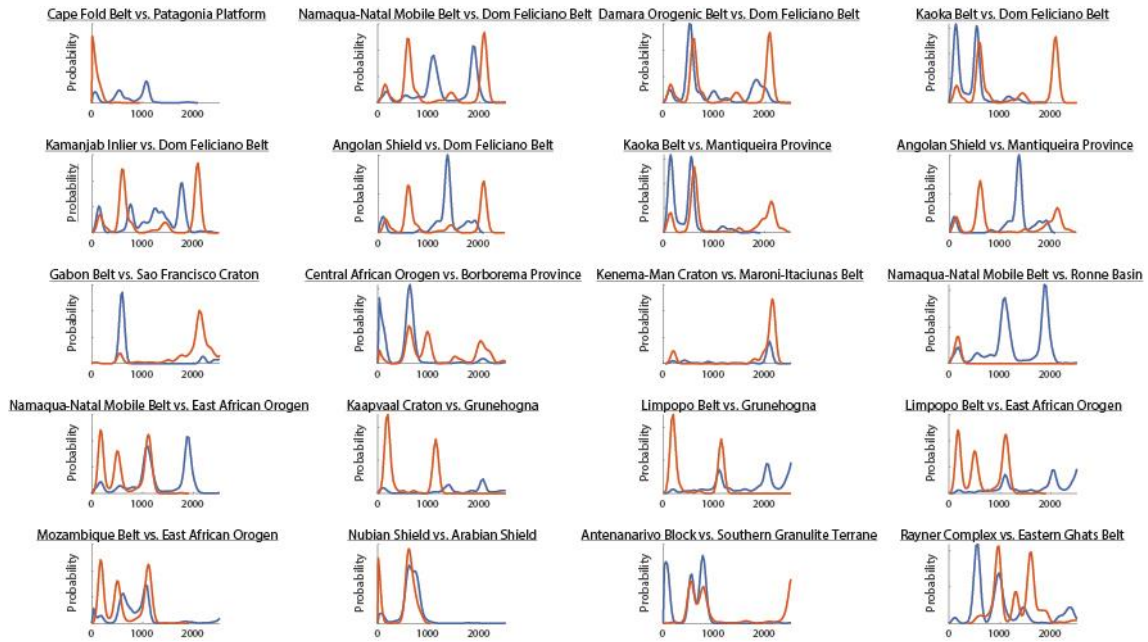


Figure 8: Kernel density plots displaying comparisons in the age distributions of the 20 most significant identified known conjugate province pairs in terms of hypothesis testing. All x-axis range from present day to 2500 Ma (data younger than age of separation was filtered out for hypothesis testing).

TWO-SAMPLE T-TEST EVALUATION

For the 20 remaining provinces, data was normalised based on province type. 20 control pairs were also normalised based on province type. All pairs were then run through two-sample t-testing. The p-values for every trace element was calculated and plotted on a histogram, in order to compare known conjugate pair p-values with control pair p-values. This is seen in Figure 9.

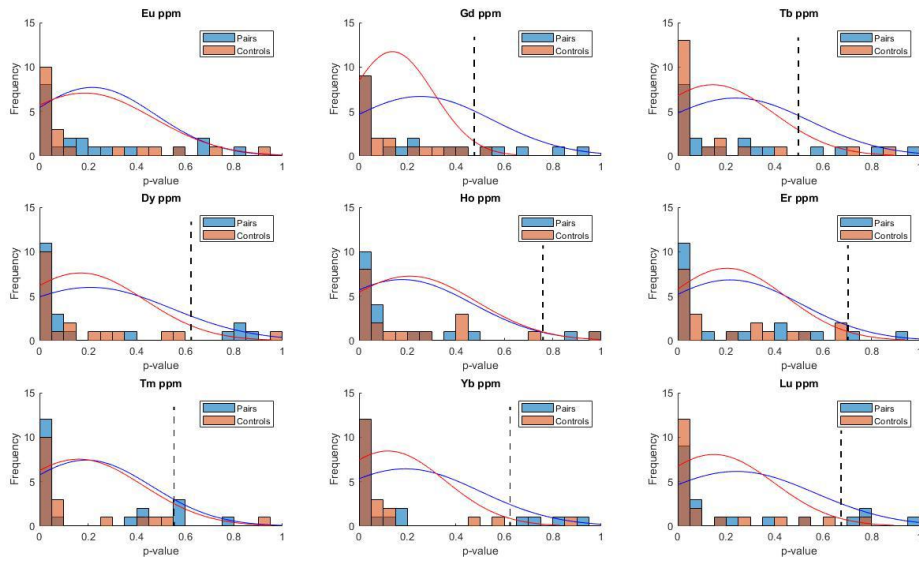


Figure 9: p-value histograms of T hypothesis testing for the Heavy Rare Earth Elements. Blue dataset signifies identified known conjugate province pairs, while orange dataset signifies random province pairing. Histograms are fitted to an ideal probability density function (blue line is known pairs, red line is controls). Identified thresholds have also been plotted (black dashed line).

All p-values for every trace element were then summed in order to calculate the known province pairs similarity ranking, relative to all other pairs. This information is seen in Figure 10.

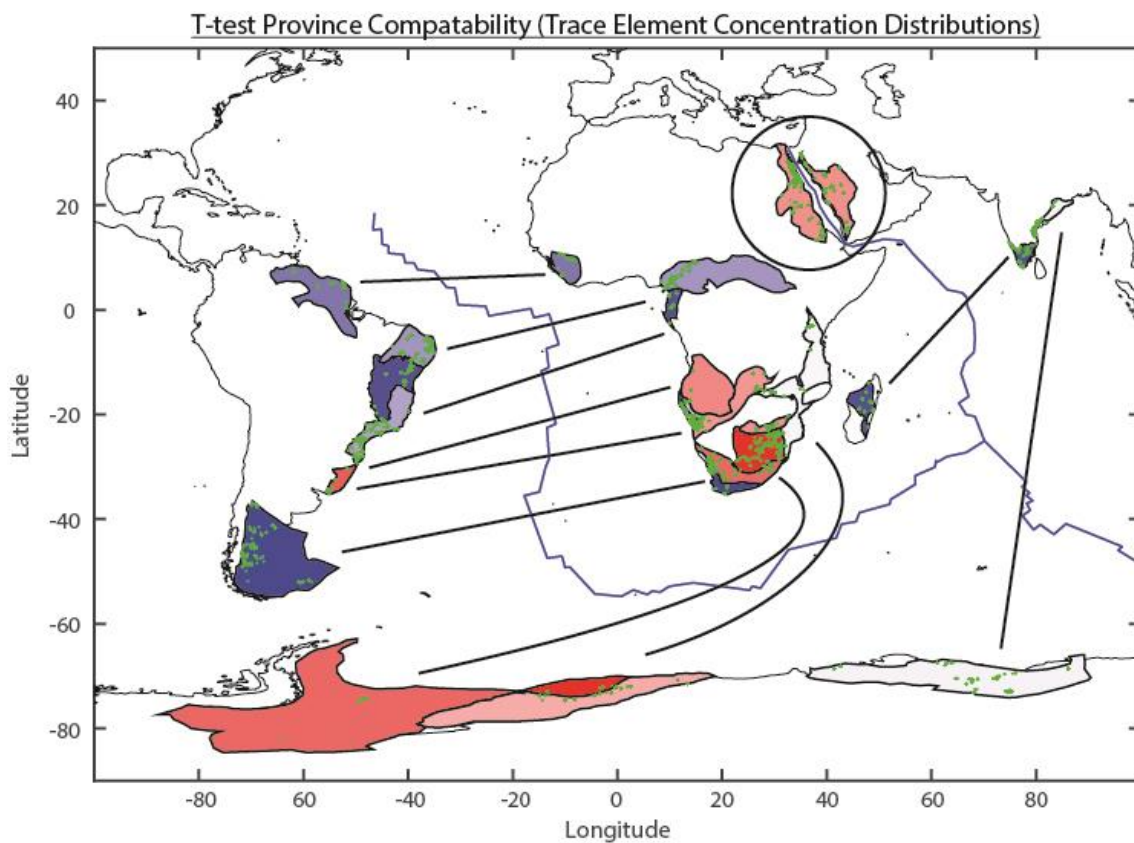


Figure 10: the 20 conjugate province pairs identified, coloured by how well their trace geochemistry distributions match relative to all other pairs (red signifies a good match, blue signifies a poorer match but are still significant matches in absolute terms). Derived from T hypothesis testing. Lines connect the pairs, while a circle highlights the Arabian-Nubian Shield pairs, an ideal case.

TWO-SAMPLE KOLMOGOROV-SMIRNOV TEST EVALUATION

The exact same methods were then carried out for the known and control province pairs but for K-S hypothesis testing. This is seen in Figures 11 and 12.

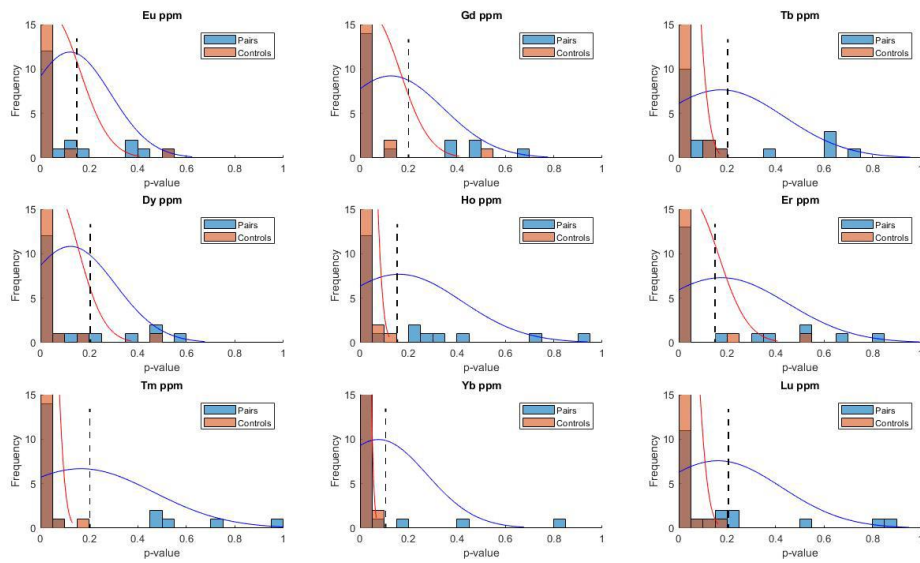


Figure 11: p-value histograms of K-S hypothesis testing for the Heavy Rare Earth Elements. Blue dataset signifies identified known conjugate province pairs, while orange dataset signifies random province pairing. Histograms are fitted to an ideal probability density function (blue line is known pairs, red line is controls). Identified thresholds have also been plotted (black dashed line).

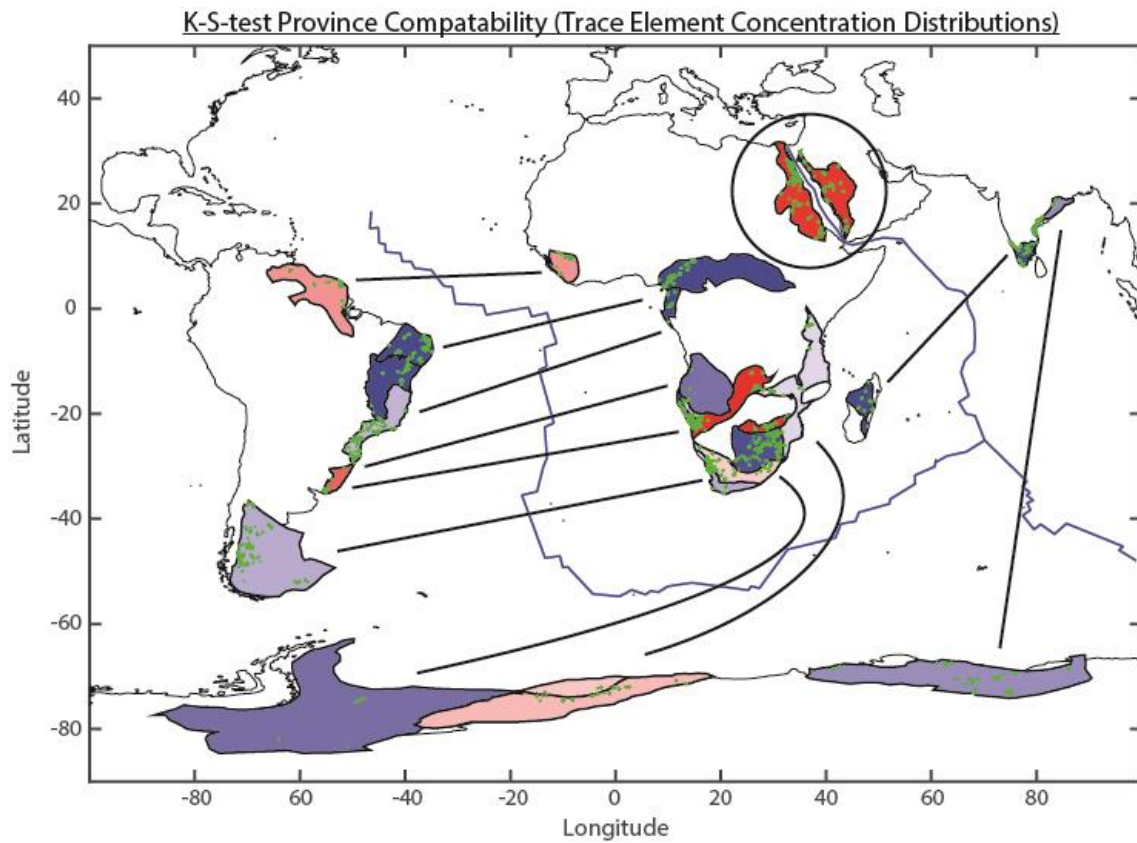


Figure 12: the 20 conjugate province pairs identified, coloured by how well their trace geochemistry distributions match relative to all other pairs (red signifies a good match, blue signifies a poorer match but are still significant matches in absolute terms). Derived from K-S hypothesis testing. Lines connect the pairs, while a circle highlights the Arabian-Nubian Shield pairs, an ideal case.

Identifying Conjugate Province Pairs for North China Craton during Nuna

NORTH CHINA CRATON HYPOTHESIS TESTING

Hypothesis testing was then carried out for all provinces which had data older than 1500 Ma (breakup of Nuna). 26 provinces successfully passed at least 10 distribution hypothesis tests based on the thresholds found earlier. A visual summary of these provinces is seen in Figure 13.

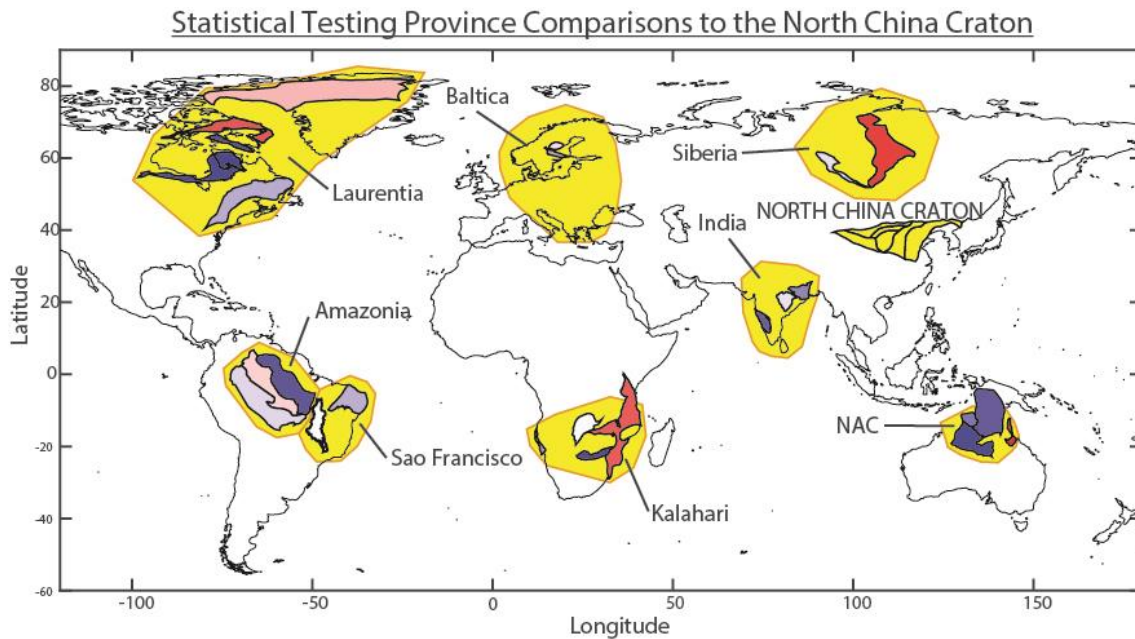


Figure 13: The 26 provinces which significantly pass both T and K-S hypothesis testing, coloured by how well their trace geochemistry distributions compare to the North China Craton provinces (red signifies a good match, blue signifies a poorer match but still passes all tests). Yellow regions are cratonic fragments of the crust which were all postulated to have been part of the Nuna supercontinent, which have been labelled.

In order to validate these identified conjugate province pairs, age distributions of all identified provinces were matched against the NCC age distributions. This is seen in Figure 14.

NORTH CHINA CRATON AGE DISTRIBUTION COMPARISONS

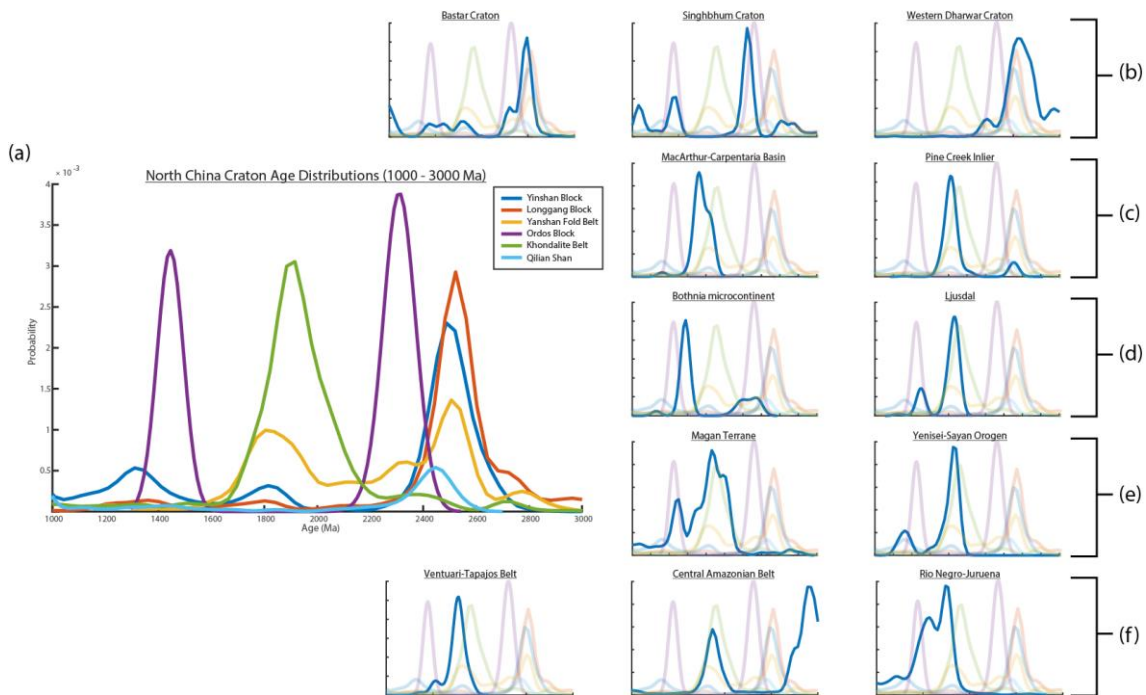


Figure 14: Kernel density plots displaying comparisons of age distributions for: a) the six provinces making up the North China Craton, b) the three Indian provinces which pass hypothesis testing, c) the two North Australian Craton provinces which pass hypothesis testing, d) the two Baltica provinces which pass hypothesis testing, e) the two Siberian provinces which pass hypothesis testing and f) the three South American provinces which pass hypothesis testing. All x-axis range from 1000 Ma to 3000 Ma.

DISCUSSION

INTERPRETATION OF NUNA CONFIGURATION RESULT

The comparison of trace element geochemistry trends in the NCC to other older tectonic provinces via hypothesis testing yielded a suitable match for 26 provinces. All of these suspected conjugate provinces are part of greater cratonic domains which are speculated to have been adjacent to the NCC during the amalgamation and stability of the supercontinent Nuna. This is given by several plate reconstruction model configurations of Nuna (de Oliveira Chaves & de Rezende, 2019). There does not seem to be a clear spatial trend in terms of which provinces are better matches geochemically. This is seen in Figure 13, where all 8 cratonic domains contain provinces which match variably to

NCC trace element distributions. Nonetheless, hypothesis testing correctly identified these province pairs. While this is a promising result, it is recognised that not all of these proposed configurations are possible and hence there must be further observations made to draw conclusion on which configuration model is the most likely.

This was done via the comparison of age distributions between the six NCC provinces and all provinces which satisfied hypothesis testing requirements. From these results, it was concluded that the North Australian Craton, Siberian, Baltica and Indian provinces were all most likely conjugate to the NCC during Nuna. The Indian province age distributions showed strong correlation to the ca. 2300 Ma and ca. 2500 Ma peaks for the NCC age data, whereas the North Australian Craton, Siberian and Baltica provinces all had age distributions which correlate to the younger NCC age peaks of ca. 1400 Ma and ca. 1800 Ma. This similarity in trace element geochemical trends but difference in temporal correlation may have implications for the movement of the NCC through time during the Paleoproterozoic, with respect to the 4 identified suspected conjugate province groups.

These results support the models proposed by (Zhang et al., 2012) and (Pisarevsky et al., 2014), as well as numerous publications looking into the NCC's connection to Nuna (Kusky et al., 2016; Li et al., 2015; Wang, 2019; Zhang et al., 2017). While the context of the NCC in relations to Nuna is well studied, it could be proposed that the results yield possible insights in the "jigsaw puzzle" that is the proposed configurations of the Nuna supercontinent (Figure 15).

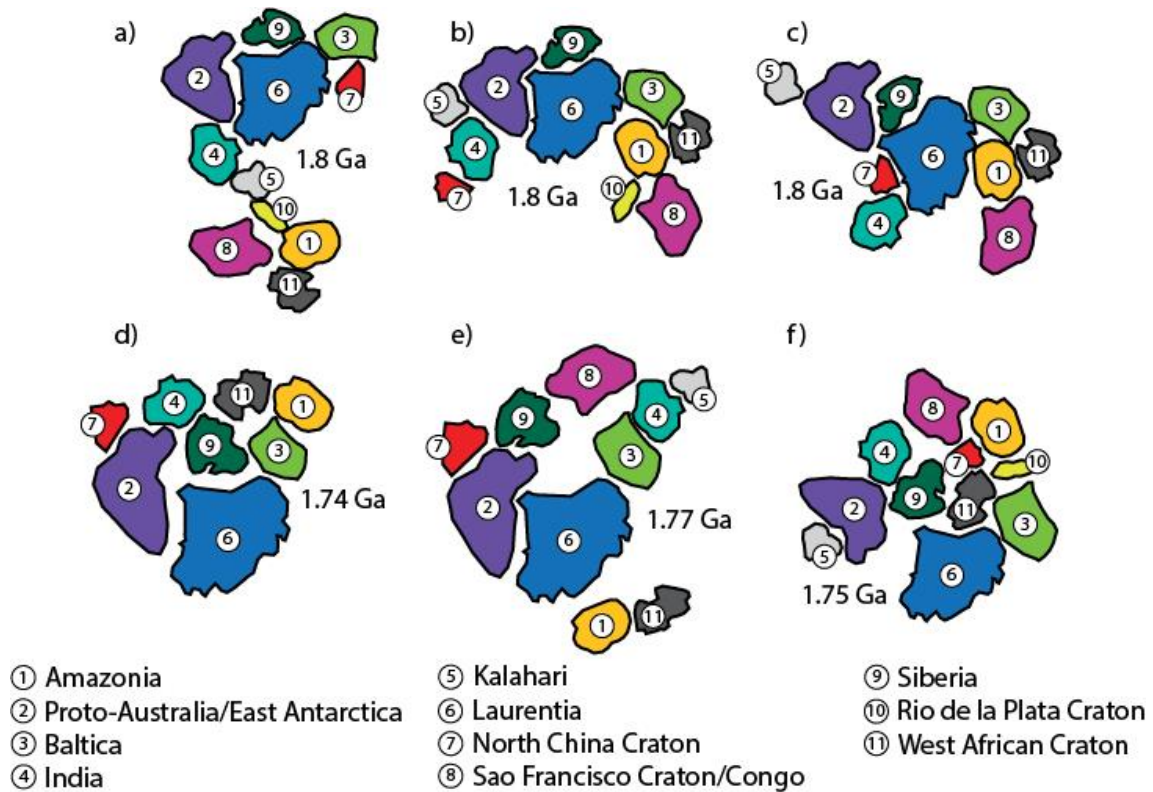


Figure 15: Several proposed relative configurations for the supercontinent Nuna (Columbia) during the late Paleoproterozoic, modified from (de Oliveira Chaves & de Rezende, 2019). Models were given by: a) (Rogers & Santosh, 2002, 2009), b) (Zhao et al., 2002; Zhao et al., 2004), c) (Hou et al., 2008), d) (Zhang et al., 2012), e) (Pisarevsky et al., 2014) and f) (de Oliveira Chaves & de Rezende, 2019).

It is important to note that for the purposes of this study, configuration resolution is limited to the province scale. “Piercing-point” methodologies provide a much more confined spatial correlation between conjugate margins, which is hence why they are so useful in plate reconstructions. However, province scale geochemical trends are much more likely to be preserved in comparison to piercing-point features.

CRITIQUE OF HYPOTHESIS TESTING

While results for the NCC’s connection to Nuna in this study suggest positive signs for the role of trace element geochemistry hypothesis testing as a form of plate reconstruction validation and improvement, the method of hypothesis testing does come

with its own limitations, the main of these being sample size limitations. Statistical analysis is entirely dependent on sample size or degrees of freedom for the datasets which it aims to interpret. Given below is the equation used to define the test statistic, t , for which the significance level (and hence p-value) can be found in a two-sample t-test.

$$t = \frac{\bar{x}_1 - \bar{x}_2}{\sqrt{s^2 \left(\frac{1}{n_1} + \frac{1}{n_2} \right)}} \text{ where } s^2 = \frac{\sum_{i=1}^{n_1} (x_i - \bar{x}_1)^2 + \sum_{j=1}^{n_2} (x_j - \bar{x}_2)^2}{n_1 + n_2 - 2} \quad (1)$$

The p-value in a hypothesis test is dependent upon the test statistic, t , and so the result of a hypothesis test correlates directly to sample size.

In the case of this study, results were strongly influenced by sample size. The filtering of data meant that some provinces only had a small number of data points available to be processed. This was the case for various Antarctic provinces, which is why constraints on similarities in trace geochemistry between Australian and Antarctic provinces was not explored, despite Australian provinces being well-sampled.

Obviously, provinces which had significantly small sample sizes (defined as being less than 50 samples) were not considered. This reduced the possible amount of known conjugate province pairs to 75, of which 20 yielded significant hypothesis testing results. In some cases, comparisons were asymmetrical in terms of sample size, meaning one size of a conjugate margin hosted more data compared to the other side, potentially biasing results. An analysis into how sample sizes affect a hypothesis test result is seen in Figure 16. Two synthetic normal distributions with the same standard deviations but slightly different means were tested, for various sample sizes. Sample size selection was based on realistic values when considering the data in conjugate province pairs in the results. Findings were that small sample sizes easily passed tests at the 95% confidence level. As sample numbers approached 50 for both sets of data,

hypothesis testing almost always failed (rejecting the null hypothesis), with the exception of an asymmetric sample size for the distributions of $N1 = 1100$ and $N2 = 20$. It can hence be determined that while asymmetry of sample sizes can affect statistical testing results, the main control is sample sizes. It is reassuring to see that testing begins to fail a sample sizes of $N1 = 50$, because this was the limit set when comparing conjugate province pairs in this study. This means that testing with sample sizes for both distributions over 50 which fail to reject the null hypothesis are much more significant in terms of the similarity between distribution means and shapes. This finding places a lot of confidence in the conjugate province pairs identified in both the validation and application parts of this study.

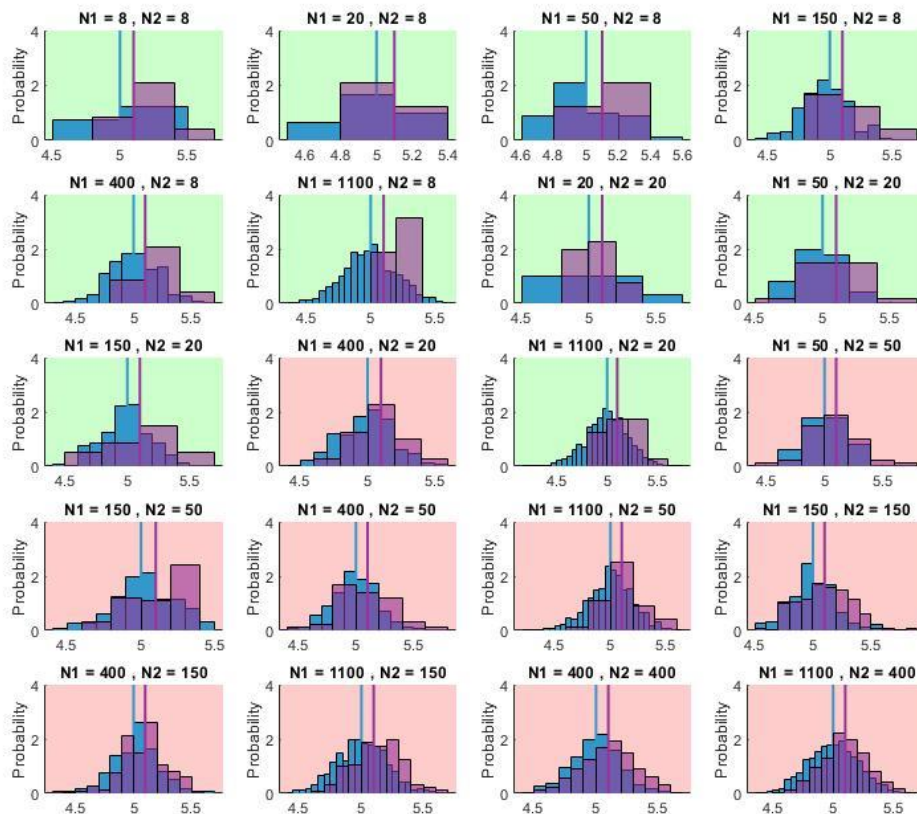


Figure 16: Hypothesis testing for two arbitrary synthetic normal distributions, with number of data for both sets changing (sample size for both distributions seen above subplots). Both distributions

have the same standard deviation (0.2), however, their means differ (blue set has a mean of 5, purple set has a mean of 5.1). Green background represents a failure to reject the null hypothesis, whereas red background represents rejection of the null hypothesis, for both T and K-S testing.

SUITABILITY OF USING GEOCHEMICAL DATA FOR PLATE RECONSTRUCTIONS

A key finding of this study is that certain trace elements are more suitable for defining trends in geochemistry than others. Of the total 39 trace elements which were analysed only 16 returned suitable and consistent test statistics. These were: Scandium, Vanadium, Yttrium, Hafnium, Tantalum, Uranium, Thorium and the heavy rare earth elements (Europium through to Lutetium). It is well known that rare earth elements are effective for comparing subtle trends in the geochemistry of igneous rocks, due to: having highly variable concentration in the Earth's crust and mantle, being relatively immobile and insoluble and presenting distinct signatures in certain tectonic environments (Rollinson, 2014). Rare earth elements share very similar physical and chemical properties but subtle differences can result in preferential fractionation in rocks and magmas. Exploiting these subtle trends in geochemistry proves invaluable when determining the genesis of certain rock species. Knowing this, comparing the distributions of rare earth element concentrations for two provinces which are assumed to have a shared genetic history should be a conclusive method. However there are a number of limitations. Firstly, a province may host rocks which shares a genetic history with the rocks hosted within its conjugate province, however these rock classifications may vary (for example, one province may host more mafic geology and its conjugate may host more felsic geology). Due to fractionation of trace elements in evolving magmas, distributions for trace elements would not share a similarity. However, the normalisation method within this study aims to overcome this problem. The

normalisation process doesn't, however, account for multiple generations of igneous activity with no genetic link.

Additionally, the scalability of distributions for trace elements is questionable, from the mineral to the province scale. Although provinces are regions of the crust which has had a consistent tectonic and genetic history, heterogeneities in trace element concentrations may “dampen-out” more distinct geochemical signatures, resulting in false similarities in two unrelated provinces (Wang & Zuo, 2020). To this end, it is perhaps more suitable to assess a particular suite or suites of rock hosted within conjugate province pairs in order to determine a more robust method for matching trace element concentration distribution similarity, which is the method traditionally used in plate reconstruction modelling (Ernst & Bleeker, 2010; Ernst et al., 2013; Williams et al., 2011).

Despite these limitations and assumptions, there are definite trends in the distributions of trace elements geochemistry for conjugate province pairs found in this study, which has implications for providing a more holistic approach to comparing geochemistry in suspected conjugate terranes in order to produce more robust plate reconstructions.

CONCLUSIONS

- There is a need to better constrain plate reconstruction models due to a number of differing configuration hypotheses in these models. Statistical methods were employed in this study to compare geochemical distributions across known and suspected province pairs as a means to provide better constraints to existing reconstruction models.

- Conjugate province pairs which had a reasonable number of data were identified for the breakup of Pangea and data was normalised by province type and compared using two-sample t and K-S testing.
- There was a subtle but statistically significant difference in identified known conjugate province pair p-values in comparison to control pair p-values, p-value thresholds of 0.5 for t-testing and 0.1 for K-S testing were defined such that p-values for the comparison between two province pair geochemical distributions which were greater than these thresholds indicate that these two province pairs likely shared a genetic and tectonic history and as such were conjugate provinces at some point in geological time (perhaps during a supercontinent phase).
- The same methods were used to assess the North China Craton's configuration during the Nuna supercontinent and it was found through hypothesis testing of geochemical distributions and age distribution validation that models which favoured the NCC as a neighbour to the North Australian Craton and either India, Siberia or Baltica also being adjacent to be the preferred models in the context of this study.
- Comparison of age distributions for suspected conjugate province pairs is an effective way to validate the reliability of hypothesis test results.
- Hypothesis testing is a highly effective method for processing large datasets and producing quantifiable rankings for the similarity between distributions, however, these statistical tests come with their own limitations.
- Overall, the use of comparing geochemistry across conjugate margins as a constraint to tectonic plate reconstruction modelling should not be

underestimated and is useful to determine the likelihood of various hypothesis for supercontinent configurations.

ACKNOWLEDGMENTS

I wish to thank first and foremost my supervisor Derrick Hasterok for his guidance and support throughout the year, without which I would never have achieved the outcomes of this project. Thanks also to my secondary supervisor Alan Collins, who provided insights into the geological side of the study. I acknowledge the Australian Research Council's Discovery Projects funding scheme (grant no. DP180104074) for financially supporting the compilation of the global geochemical database. Lastly, my deepest gratitude goes out to my fellow honours cohort, especially Alisha de Groot, Caelan Grooby, Erica van der Wolff, Zara Woolston, Brooke North, Kelly Macdonald, Samantha March, Peter Keller and Elyse Bosch for providing unconditional support and for making a challenging year all the more worth it.

REFERENCES

- Brookfield, M. (1993). Neoproterozoic Laurentia-Australia fit. *Geology*, 21(8), 683-686.
- Burrett, C., & Berry, R. (2000). Proterozoic Australia–Western United States (AUSWUS) fit between Laurentia and Australia. *Geology*, 28(2), 103-106.
- Cawood, P. A., Kroner, A., & Pisarevsky, S. (2006). Precambrian plate tectonics: criteria and evidence. *GSA today*, 16(7), 4.
- Condie, K. C. (2002). The supercontinent cycle: are there two patterns of cyclicity? *Journal of African Earth Sciences*, 35(2), 179-183.
- Dalziel, I. W. (1997). OVERVIEW: Neoproterozoic-Paleozoic geography and tectonics: Review, hypothesis, environmental speculation. *Geological Society of America Bulletin*, 109(1), 16-42.
- de Oliveira Chaves, A., & de Rezende, C. R. (2019). Fragments of 1.79-1.75 Ga Large Igneous Provinces in reconstructing Columbia (Nuna): a Statherian supercontinent-superplume coupling? *Episodes Journal of International Geoscience*, 42(1), 55-67.
- Domeier, M., & Torsvik, T. H. (2014). Plate tectonics in the late Paleozoic. *Geoscience Frontiers*, 5(3), 303-350.
- Ernst, R., & Bleeker, W. (2010). Large igneous provinces (LIPs), giant dyke swarms, and mantle plumes: significance for breakup events within Canada and adjacent regions from 2.5 Ga to the Present. *Canadian Journal of Earth Sciences*, 47(5), 695-739.
- [Record #38 is using a reference type undefined in this output style.]
- Evans, D., Li, Z.-X., & Murphy, J. (2016). Four-dimensional context of Earth's supercontinents. *Geological Society, London, Special Publications*, 424(1), 1-14.

- Evans, D. A. (2013). Reconstructing pre-Pangean supercontinents. *Bulletin*, 125(11-12), 1735-1751.
- Gard, M., Hasterok, D., & Halpin, J. A. (2019). Global whole-rock geochemical database compilation.
- Hasterok, D., Gard, M., Bishop, C., & Kelsey, D. (2019). Chemical identification of metamorphic protoliths using machine learning methods. *Computers & Geosciences*, 132, 56-68.
- Hasterok, D., & Webb, J. (2017). On the radiogenic heat production of igneous rocks. *Geoscience Frontiers*, 8(5), 919-940.
- Haus, M., & Pauk, T. (1993). *PETROCH lithochemochemical data*. Ministry of Northern Development & Mines, Ontario Geological Survey.
- Hoffman, P. F. (1991). Did the breakout of Laurentia turn Gondwanaland inside-out? *Science*, 252(5011), 1409-1412.
- Honarvar, P., Nolan, L., Crisby-Whittle, L., & Morgan, K. (2013). The geoscience atlas. *Report 13-1, Newfoundland and Labrador Department of Natural Resources, 2013. Geological Survey*.
- Hou, G., Santosh, M., Qian, X., Lister, G. S., & Li, J. (2008). Configuration of the Late Paleoproterozoic supercontinent Columbia: insights from radiating mafic dyke swarms. *Gondwana Research*, 14(3), 395-409.
- Karlstrom, K. E., Harlan, S. S., Williams, M. L., McLelland, J., Geissman, J. W., & Ahall, K.-I. (1999). Refining Rodinia: Geologic evidence for the Australia–western US connection in the Proterozoic. *GSA today*, 9(10), 1-7.
- Kusky, T., Polat, A., Windley, B. F., Burke, K., Dewey, J., Kidd, W., Maruyama, S., Wang, J., Deng, H., & Wang, Z. (2016). Insights into the tectonic evolution of the North China Craton through comparative tectonic analysis: A record of outward growth of Precambrian continents. *Earth-Science Reviews*, 162, 387-432.
- Li, C., Chen, D., Chen, J., Chen, X., Yang, X., & Aboelnour, M. (2015). Correlations between the North China Craton and the Indian Shield: Constraints from regional metallogeny. *Geoscience Frontiers*, 6(6), 861-873.
- Li, Z.-X., Bogdanova, S., Collins, A., Davidson, A., De Waele, B., Ernst, R., Fitzsimons, I., Fuck, R., Gladkochub, D., & Jacobs, J. (2008). Assembly, configuration, and break-up history of Rodinia: a synthesis. *Precambrian research*, 160(1-2), 179-210.
- Li, Z.-X., Zhang, L., & Powell, C. M. (1995). South China in Rodinia: part of the missing link between Australia–East Antarctica and Laurentia? *Geology*, 23(5), 407-410.
- Merdith, A. S., Collins, A. S., Williams, S. E., Pisarevsky, S., Foden, J. D., Archibald, D. B., Blades, M. L., Alessio, B. L., Armistead, S., & Plavsa, D. (2017). A full-plate global reconstruction of the Neoproterozoic. *Gondwana Research*, 50, 84-134.
- Merdith, A. S., Williams, S. E., Brune, S., Collins, A. S., & Müller, R. D. (2019). Rift and plate boundary evolution across two supercontinent cycles. *Global and planetary change*, 173, 1-14.
- Moore, E. (1991). Southwest US-East Antarctic (SWEAT) connection: a hypothesis. *Geology*, 19(5), 425-428.

- Nance, R. D., Murphy, J. B., & Santosh, M. (2014). The supercontinent cycle: a retrospective essay. *Gondwana Research*, 25(1), 4-29.
- Newfoundland, Survey, L. G., & Davenport, P. (1999). *Digital Geoscience Atlas of Labrador*. Geological Survey, Government of Newfoundland and Labrador.
- Pisarevsky, S. A., Elming, S.-Å., Pesonen, L. J., & Li, Z.-X. (2014). Mesoproterozoic paleogeography: supercontinent and beyond. *Precambrian research*, 244, 207-225.
- Puetz, S. J. (2018). A relational database of global U–Pb ages. *Geoscience Frontiers*, 9(3), 877-891.
- Rogers, J. J., & Santosh, M. (2002). Configuration of Columbia, a Mesoproterozoic supercontinent. *Gondwana Research*, 5(1), 5-22.
- Rogers, J. J., & Santosh, M. (2003). Supercontinents in Earth history. *Gondwana Research*, 6(3), 357-368.
- Rogers, J. J., & Santosh, M. (2009). Tectonics and surface effects of the supercontinent Columbia. *Gondwana Research*, 15(3-4), 373-380.
- Rollinson, H. R. (2014). *Using geochemical data: evaluation, presentation, interpretation*. Routledge.
- Salminen, J. (2009). Paleomagnetic and rock magnetic study with emphasis on the Precambrian intrusions and impact structures in Fennoscandia and South Africa.
- Sarbas, B. (2008). The GEOROC database as part of a growing geoinformatics network. Geoinformatics 2008—Data to Knowledge,
- Schiffer, C., Stephenson, R. A., Petersen, K. D., Nielsen, S. B., Jacobsen, B. H., Balling, N., & Macdonald, D. I. (2015). A sub-crustal piercing point for North Atlantic reconstructions and tectonic implications. *Geology*, 43(12), 1087-1090.
- Verard, C. (2019). Plate tectonic modelling: review and perspectives. *Geological Magazine*, 156(2), 208-241.
- Wang, C. (2019). *Paleogeographic reconstruction of the North China Craton in the supercontinent Nuna/Columbia: paleomagnetic and geological constraints* [Curtin University].
- Wang, J., & Zuo, R. (2020). Quantifying the Distribution Characteristics of Geochemical Elements and Identifying Their Associations in Southwestern Fujian Province, China. *Minerals*, 10(2), 183.
- White, L. T., Gibson, G. M., & Lister, G. S. (2013). A reassessment of paleogeographic reconstructions of eastern Gondwana: Bringing geology back into the equation. *Gondwana Research*, 24(3-4), 984-998.
- Williams, S. E., Whittaker, J. M., & Müller, R. D. (2011). Full-fit, palinspastic reconstruction of the conjugate Australian-Antarctic margins. *Tectonics*, 30(6).
- Wingate, M. T., & Giddings, J. W. (2000). Age and palaeomagnetism of the Mundine Well dyke swarm, Western Australia: implications for an Australia–Laurentia connection at 755 Ma. *Precambrian research*, 100(1-3), 335-357.
- Yoshida, M., & Santosh, M. (2011). Supercontinents, mantle dynamics and plate tectonics: a perspective based on conceptual vs. numerical models. *Earth-Science Reviews*, 105(1-2), 1-24.
- Zhang, S.-H., Zhao, Y., Li, X.-H., Ernst, R. E., & Yang, Z.-Y. (2017). The 1.33–1.30 Ga Yanliao large igneous province in the North China Craton: Implications for

reconstruction of the Nuna (Columbia) supercontinent, and specifically with the North Australian Craton. *Earth and Planetary Science Letters*, 465, 112-125.

- Zhang, S., Li, Z.-X., Evans, D. A., Wu, H., Li, H., & Dong, J. (2012). Pre-Rodinia supercontinent Nuna shaping up: a global synthesis with new paleomagnetic results from North China. *Earth and Planetary Science Letters*, 353, 145-155.
- Zhao, G., Cawood, P. A., Wilde, S. A., & Sun, M. (2002). Review of global 2.1–1.8 Ga orogens: implications for a pre-Rodinia supercontinent. *Earth-Science Reviews*, 59(1-4), 125-162.
- Zhao, G., Sun, M., Wilde, S. A., & Li, S. (2004). A Paleo-Mesoproterozoic supercontinent: assembly, growth and breakup. *Earth-Science Reviews*, 67(1-2), 91-123.